4.3 Loading Tests

1) Test Methods

Various loading tests are used to determine element properties which are not evaluated based on theoretical procedures or verifying the theoretical procedures. Depending on the size of specimens, there are prototype test and scaled model test. Since the prototype test is not easy to conduct because of large size of actual bridge piers, scaled model test is generally conducted.

In the scaled model test, models have to be carefully planned and designed considering the similarity rule and the capacity of testing facility. How strictly the models should be scaled down depends on how the test results are used. If one wants to evaluate the capacity of a prototype based on a test for the scaled models, the similarity rule has to be strictly considered. On the other hand, if one wants to analyze the test results to verify the analytical model, the models can be so designed and constructed that the models capture the features of failure modes of the prototype. In this case, it is not necessary to strictly consider the similarity rule as long as the properties of the model are known. The capacity of a prototype can be estimated using the analytical method which was proved by the scaled model test.

In reinforced concrete piers/columns, there are various factors to be included in the design of models. Size of aggregates is important because spalling of core concrete is restricted if the aggregate size is too large compared to the space of longitudinal bars and hoops. Diameter of longitudinal bars affects the buckling strength of longitudinal bars. As a consequence, using longitudinal bars with larger bar diameter yields longer plastic hinge length resulting in larger displacement capacity. This implies that only scaling down the size of a model by the geometrical scale is not sufficient to bars. Because bucking strength of bars depends on the flexural rigidity, it may be an idea to scale down the bars by the scale of the flexural rigidity. However there are many unknowns on the scaling, and the scaling depends on each researcher at this moment. There is a movement to synthesize the testing procedures for bridge piers (Federal Highway Administration 2002, Yen, P. 2002).

Tests can be classified into *quasi-static test* and *dynamic test* from the loading rate. In the quasi-static test, a test is conducted between tens of minutes and 1 day. The test has to be conducted with a loading rate where the creep effect and the slow bond failure effect become predominant. In the dynamic loading test, loads are generally applied to a model with the real loading rate.

In the quasi-static test, there are monotonic loading tests (pushover tests), cyclic loading tests, and hybrid loading tests. The monotonic loading test is conducted for evaluating basic hysteretic behavior of a structure or structural elements. The cyclic loading tests are most commonly used to know hysteretic behavior under cyclic load. Maximum strength, maximum displacement, unloading and reloading paths are generally obtained. It is common to stepwise increase loading amplitude under the displacement control. Number of load cycle per step and increment of loading amplitude are important parameters in the cyclic loading test, but they are not yet unified.

The hybrid loading method is a hybrid of a loading test and a numerical analysis. A part of a structural system where the plastic deformation occurs is idealized by a test model with the rest of the structural system being idealized by an analytical model. The test and analysis are conducted by a stepwise direct integration. Obtaining a restoring force $R(t)$ at time t by the model test, the equations of motion of the system, after incorporating $R(t)$ at an appropriate location in the equations, are solved for response displacement at time $t+\Delta t$. Then this displacement is applied to the model by an actuator, and the restoring force $R(t+\Delta t)$ at time $t+\Delta t$ is measured. By repeating this process, one can obtain the seismic response of the structural system. Benefit of the hybrid loading test is that one can evaluate seismic response of a structural system without using a shake table. However, since it takes time for the process of getting measured restoring force, computing response at the next time step, and prescribing this displacement to the model, the test is conducted in a quasi-static manner. It is common that the time required for a test is 100-200 times the real time. However, various researches are going on for real-time hybrid loading tests.

2) Yield and Ultimate

Fig. 4.14 shows an example of how failure of a reinforced concrete column progresses under a cyclic load reversal. The column is 1.75 m tall and has a 400 mm x 400 mm square section. The column is loaded in the A-B direction at 1.35 m from the bottom (effective height) by a horizontal actuator (attached at A) using a step-wide increasing loading hysteresis. The lateral displacement is increased 0.5% drift, 1% drift, 1.5% drift,….. until failure. Three load reversal is applied at each loading step. Before conducting the first step load excursion with 0.5% drift displacement, the column is loaded with an amplitude of 0.5% drift so that fitting of specimen and loading facility is guaranteed. A constant vertical force of 160 kN, which results in a stress of 1MPa, is applied by a vertical actuator. After 1% drift loading, the column has several horizontal flexural cracks. After 2% drift loading, the cracks progress and several diagonal cracks are generated. Concrete at the bottom corners starts to spall off. After 3% drift loading, the spall off of concrete at the bottom corners extensively spalled off due to flexural compression. After 4% drift loading, the covering concrete spalled off completely, and extensive local buckling of longitudinal bars occur. The ties deformed outward direction which shows that the confinement of core concrete is almost lost. A longitudinal bar ruptures during the 4% drift loading.

In a typical column which fails in flexure, the damage progresses from flexural cracks and progresses to flexural failure of concrete, outward buckling of longitudinal bars, outward deformation of ties, spall off of covering concrete, and rupture of longitudinal and tie bars.

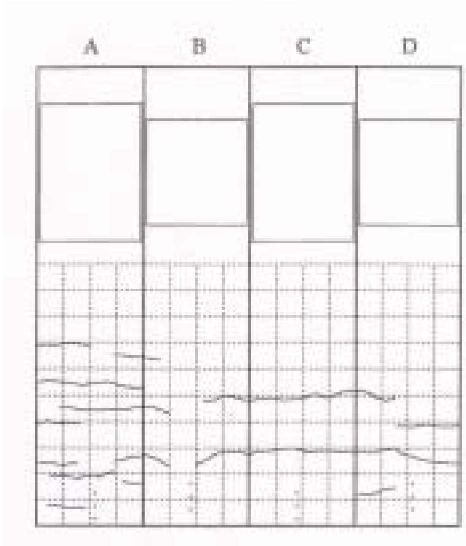

(a) Drift 1%

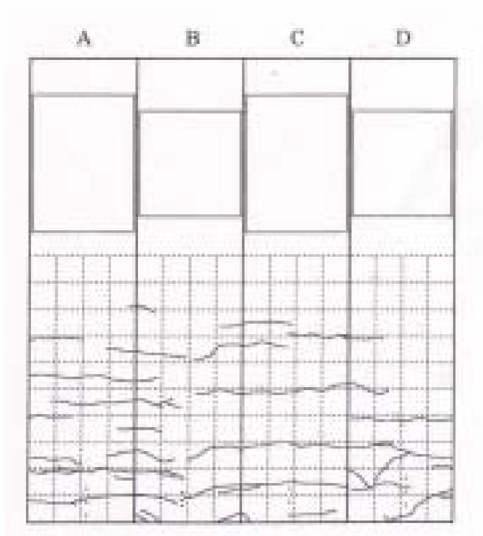

(b) Drift 2%

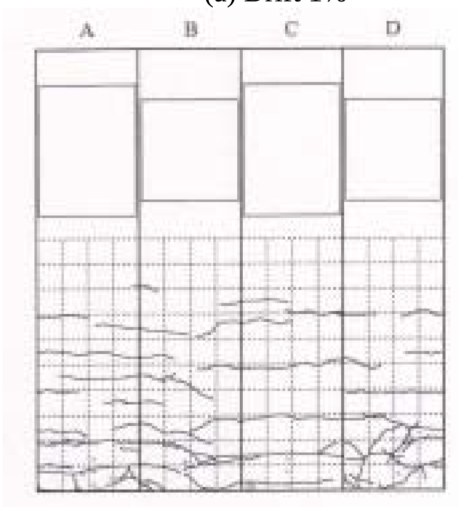

(c) Drift 3%

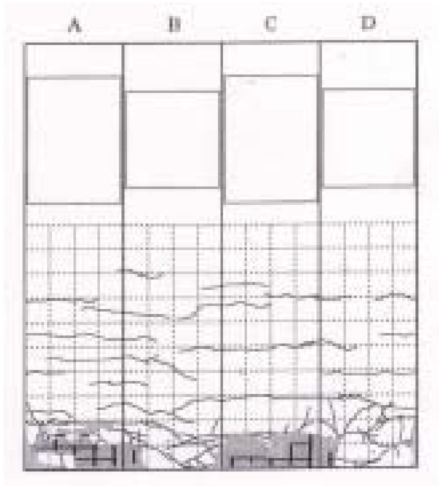

(d) Drift 4%

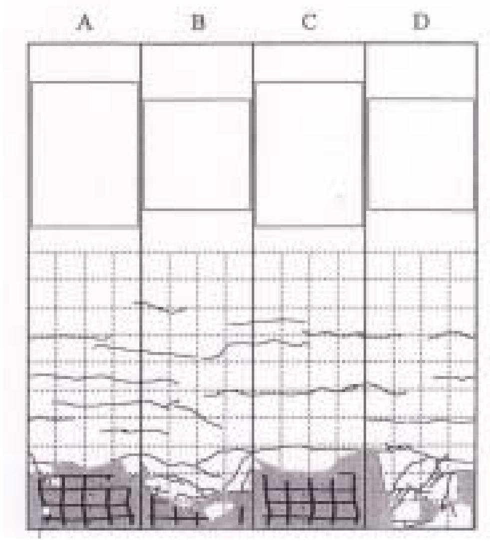

(f) Drift 5%

Fig.4.14 Progress of Failure under Cyclic Loading

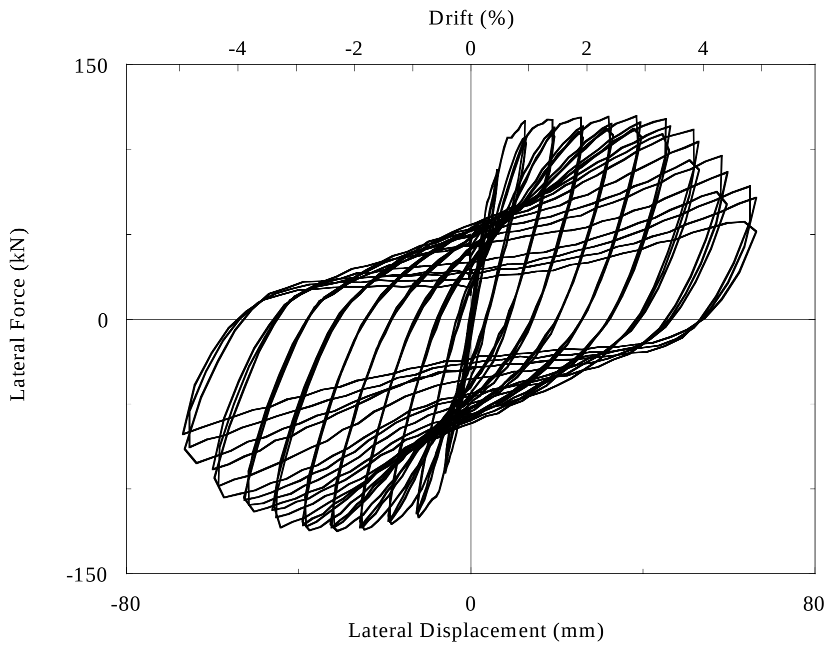

Fig.4.15 Lateral Force vs. Lateral Displacement Hysteresis

Fig. 4.15 shows the lateral force vs. lateral displacement hysteresis of this column. As the lateral displacement increases the lateral load increases at the first stage. The lateral force becomes saturated at about 1% drift and keeps this force level (flexural strength P_y) until 4% drift. The lateral force significantly decreases over 4.5% drift. Stiffness of unloading and reloading paths from the peak displacements gradually deteriorates as the lateral displacement increases.

Fig. 4.16 idealizes an envelop of the lateral force vs. lateral displacement hysteresis. The

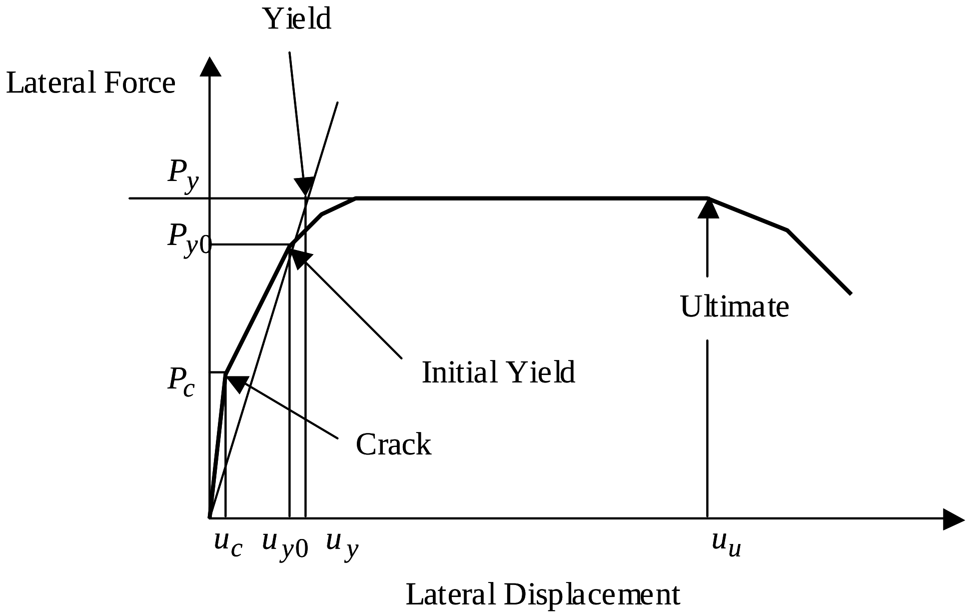

Fig.4.16 First Yield, Yield, and Ultimate of a Column which fails in Flexure

column has at first the uncracked stiffness defined as

$$k_{uc} = \frac{P_c}{u_c} \tag{4.69}$$

where P_c and u_c represent the lateral force and the lateral displacement when flexural cracks first occur. Yield of the column starts when rebars at the extreme fiber in compression yield at P_{y0} and u_{y0}. This is called initial yield. The cracked stiffness of the column is defined as

$$k_{cr} = \frac{P_{y0}}{u_{y0}} \tag{4.70}$$

As the lateral displacement increases, other rebars next to the rebars at the extreme fiber start to yield, and the lateral force is eventually saturated at P_y (flexural strength) when all rebars in the flexural compression zone yield. There are various ways of defining yield of a column. However, it is common to define it as an intersection between a line connecting the original rest point and the initial yield and a line of the flexural strength.

Significant deterioration of lateral force occurs when one of the following failures occurs; (1) spalling off of covering concrete, (2) local buckling of longitudinal rebars, (3) extensive outward deformation of ties, and (4) rupture of longitudinal rebars. Although the local buckling of rebars cannot be identified from the surface of a column at the early loading stage, it is likely that the rebars have already buckled when the covering concrete starts to spall off. Deformation of rebars due to the local buckling pushes the covering concrete, which accelerates the covering concrete to spall off. Ultimate of a column is generally defined as a stage when the column exhibits an extensive deterioration of restoring force. Denoting the ultimate displacement of a column as u_u, displacement ductility capacity of a column μ_d is defined as

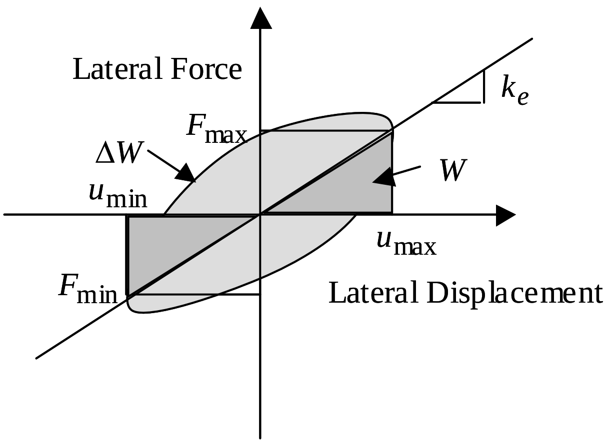

Fig.4.16 Equivalent Stiffness and Energy Dissipation

$$\mu_d = \frac{u_u}{u_y} \tag{4.71}$$

3) Equivalent Stiffness and Energy Dissipation

As shown in Fig. 4.16, an equivalent stiffness of a column may be defined for each loading step as

$$k_e = \frac{P_{\max} - P_{\min}}{u_{\max} - u_{\min}} \tag{4.72}$$

where $u_{\max}$ and $u_{\min}$ represent the maximum and minimum displacements on a hysteresis loop, and $F_{\max}$ and $F_{\min}$ represent the restoring forces at $u_{\max}$ and $u_{\min}$. Fig. 4.17 shows how the equivalent stiffness k_e deteriorates as the lateral displacement increases.

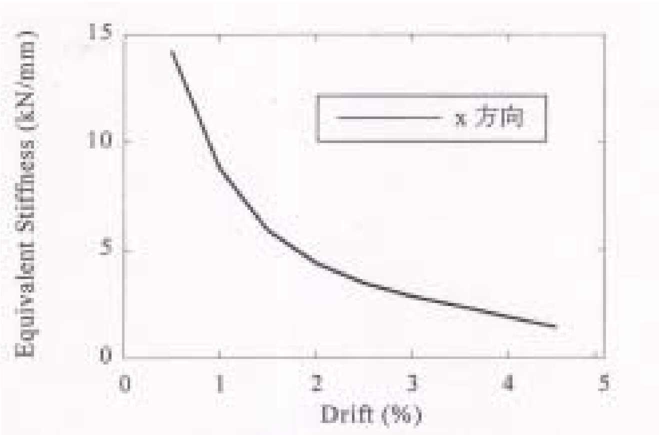

Fig.4.17 Deterioration of Equivalent Stiffness

On the other hand, energy dissipated during an i-th load reversal is evaluated as

$$\Delta W_i = \int_{-u_{\min}}^{u_{\max}} F_l(u)du + \int_{u_{\max}}^{-u_{\min}} F_{ul}(u)du = \int_{-u_{\min}}^{u_{\max}} (F_l(u) - F_{ul}(u))du \tag{4.73}$$

where $F_l(u)$ and $F_{ul}(u)$ represent the force at displacement u during loading and unloading processes. As shown in Fig. 4.16, ΔW_i by Eq. (4.73) represents the area of surrounded by a hysteresis. The accumulated energy dissipated in a column is then obtained as

$$\Delta W = \sum_i \Delta W_i \tag{4.74}$$

Defining a strain energy W as shown in Fig. 4.16, an equivalent damping ratio of a column can be written as

$$\xi_e = \frac{\Delta W}{2\pi W} \tag{4.75}$$

where

$$W = \frac{k_e}{2}\left(u_{\max}{}^2 + u_{\min}{}^2\right) \tag{4.76}$$

Fig. 4.18 shows the energy dissipation at each loading step ΔW_i, the accumulated energy dissipation ΔW, and the equivalent damping ratio ξ_e, by Eqs. (4.73), (4.74), and (4.75), respectively, for the column presented in Fig. 4.15. The energy dissipation capacity ΔW_i is maximum between 4 and 4.5% drift, and then it sharply decreases since the rupture of longitudinal rebars progressed. The column dissipated energy with an amount of 150 kNm. The accumulated energy ΔW is an index of an energy dissipating capacity of a column.

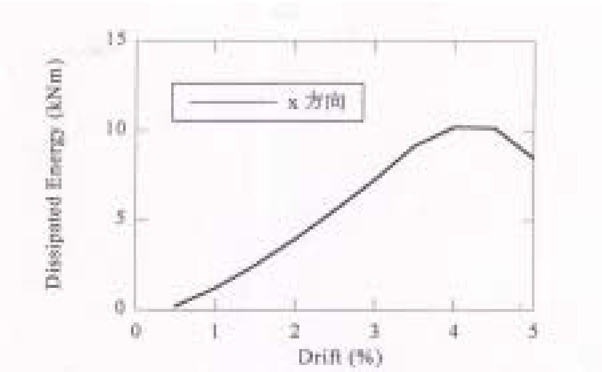

(a) Energy Dissipation ΔW_i

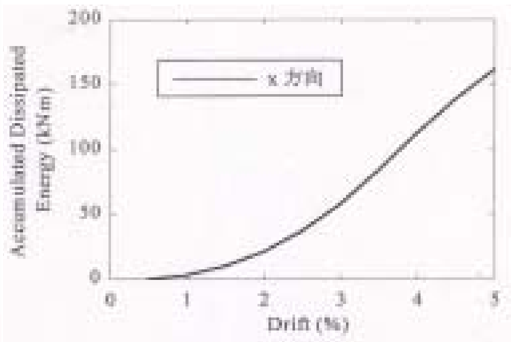

(b) Accumulated Energy Dissipation ΔW

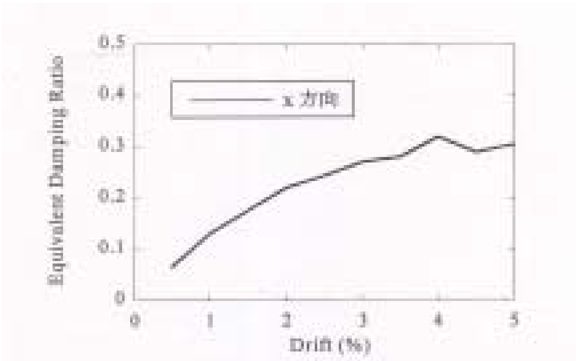

(c) Equivalent Damping Ratio

Fig.4.18 Energy Dissipation and Equivalent Damping Ratio

4.6 Effect of Various Factors on Strength and Ductility Capacities of Reinforced Concrete Columns

1) Effect of Loading Hysteresis

A stepwise increase loading scheme provides information of hysteretic behavior of structural members under a gradual increase of seismic load. However under a near-field ground excitation, a structural member is subjected to a large lateral force in the early moment nearly without a step of gradual increase. A stepwise decrease loading scheme may provide information of hysteretic behavior of a structural member under such an excitation. It is therefore interesting to know the effect of loading hysteresis on the hysteretic performance of reinforced concrete columns.

A stepwise decrease and increase loading test provides the effect of loading hysteresis. A test was conducted for two 1.35 m tall (effective height) circular reinforced concrete columns with a diameter of 400mm. Twenty deformed bars with a diameter of 13 mm (D13) and D6 bars at a 50mm interval are provided for longitudinal and tie bars, respectively. Longitudinal reinforcement ratio and tie (volumetric) reinforcement ratio are 2.02% and 0.745%, respectively. Concrete strength is 22.4 MPa. In the stepwise increase loading, displacement in increased from 0.5% drift with an increment of 0.5% drift. Since the yield displacement is 14.5 mm, 1% drift (13.5 mm) corresponds to 1.1 times yield displacement. On the other hand,

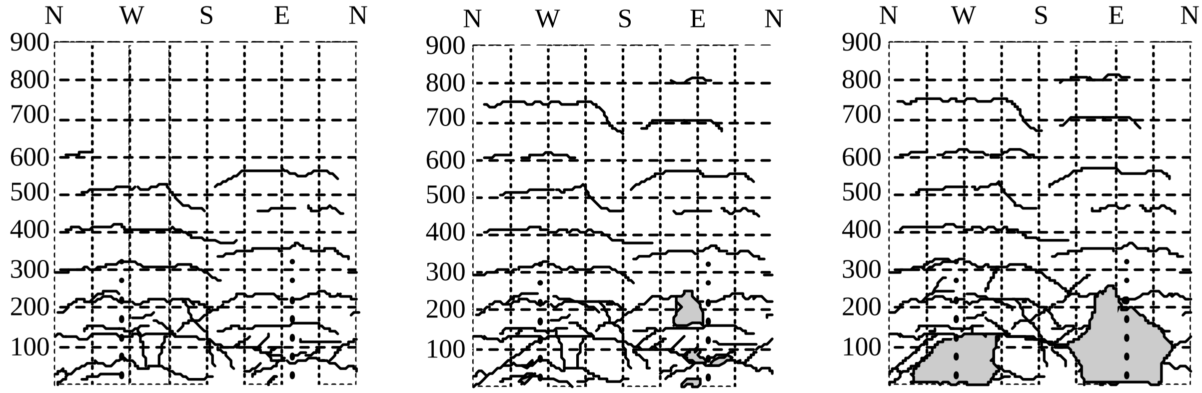

(a) Drift 3.5% (b) Drift 4.5% (c) Drift 6.0%

(1) Stepwise Increasing Loading

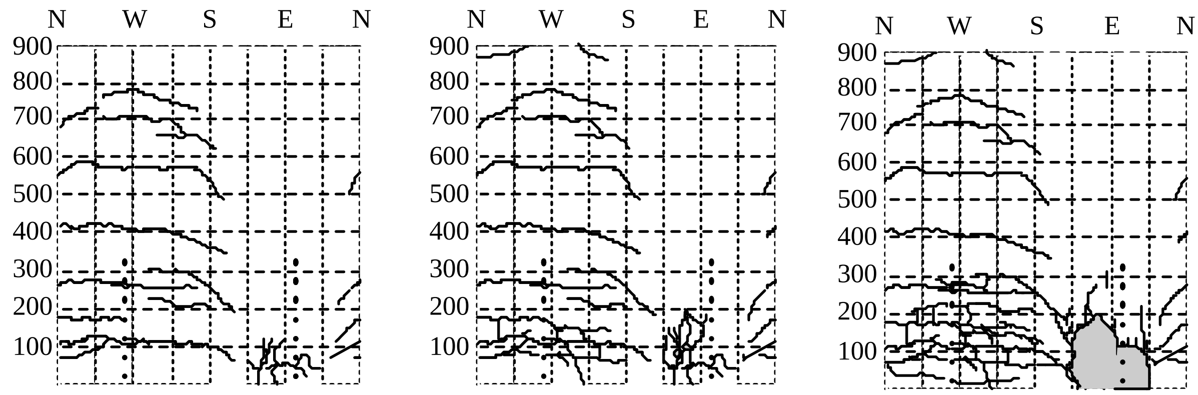

(a) Drift +2.8% (b) Drift +4.1% (c) Drift +5.5%

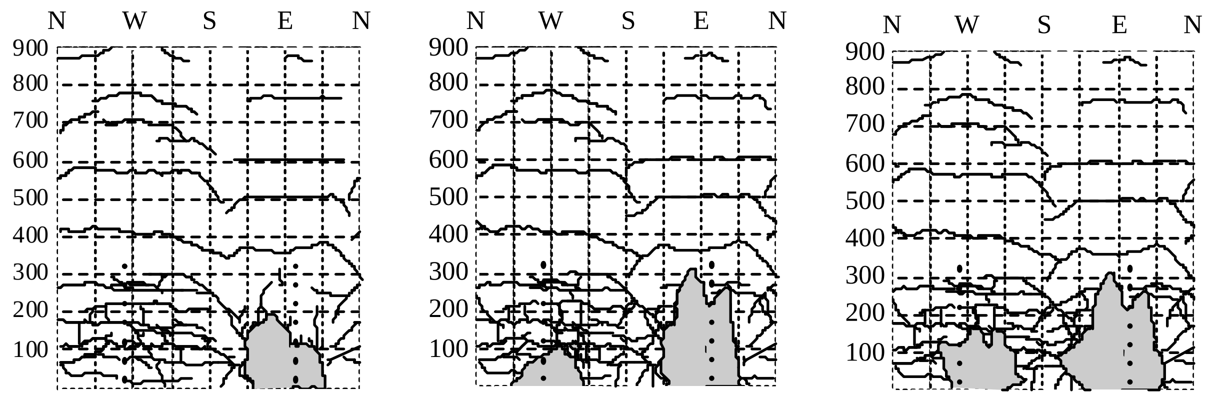

(d) Drift –2.2% (e) Drift –5.2% (f) Drift 4.5%

(2) Stepwise Decreasing Loading

Fig.4.19 Failure Modes

in the stepwise decrease loading, the loading displacement is decreased from 6% with an increment of 0.5% drift.

Fig. 4.19 compares the progress of failure at typical loading displacements between the stepwise decrease and increase loading schemes. Both columns were loaded in E-W direction. In the stepwise increase loading, extensive flexural cracks have occurred until 3.5% drift loading. At 4.5% drift, covering concrete at E surface starts to spall off, and extensive spall off of the covering concrete has occurred at both surfaces until the end of 6% drift loading. On the other hand, in the stepwise decrease loading, extensive tension cracks and compression failure occur at the tension side (W) and compression side (E), respectively, at 2.8%, 4.1% and 5.5% drifts on the first load excursion toward 6% drift. Since the column is simply pushed in the E direction during the first load excursion, it is a pushover test. During -2.2% and -5.2% drift loadings on the subsequent excursion toward -5.5% drift, compression failure start to occur at W surface (compression) and the compression failure at E surface which has occurred in the first loading excursion toward 6% drift progresses. By 4.5% drift loading on the third excursion toward 5% drift, failure of covering concrete has occurred extensively on both W and E surfaces. This failure mode is similar to the failure after 6% drift loading in the stepwise increase loading (refer to Fig. 4.19 (1) (c)).

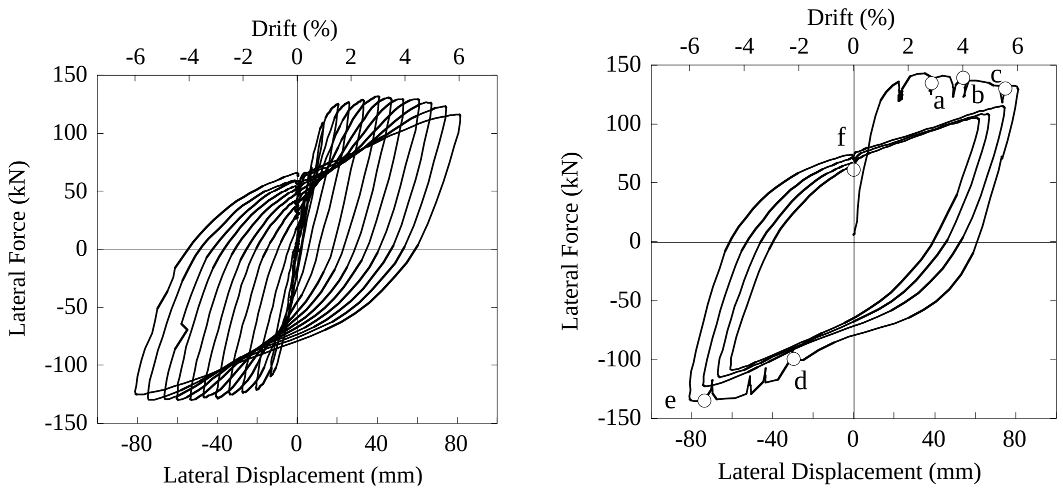

(a) Stepwise Increase Loading (b) Stepwise Decrease Loading

Fig.4.20 Effect of Loading Scheme on the Lateral Force vs. Lateral Displacement Hystereses

Fig. 4.20 shows the hystereses of the lateral force vs. lateral displacement relation for both the specimens. Symbols from “a” to “f” in Fig. 4.20 (b) correspond to Fig. 4.19 (2). Small decrease of the lateral force at several loading displacements of the column subjected to the stepwise decrease scheme resulted from pause of loading to observe damage. Fig. 4.21 compares envelops of the two hystereses. The hystereses are similar for both the stepwise decrease and increase loadings although the lateral force is slightly larger in the column subjected to the stepwise decrease loading than the column subjected to the stepwise increase loading. The restoring force at the virgin excursion may be larger than the restoring force after experiencing several load reversals.

In the above example, the effect of loading hysteresis is limited. Since the columns have a circular section, deterioration of restoring force is limited. However the effect of loading

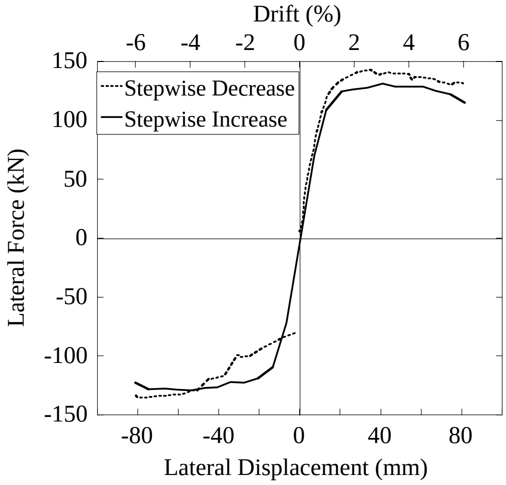

Fig.4.21 Comparison of Envelopes of Lateral Force vs. Lateral Displacement Hystereses

hysteresis may be more significant in rectangular columns. The similar test was conducted for six 1.245 m tall (effective height) rectangular reinforced concrete columns with a section of 400 mm x 400 mm. Twenty D13 are provided for longitudinal bars, and D6 bars are provided with 70 mm interval for ties. Therefore the longitudinal reinforcement ratio and the volumetric tie reinforcement ratio are 1.58% and 0.79%, respectively. The concrete strength is between 33.2 and 36.8 MPa. A constant axial force of 156.8 kN is applied, which results in

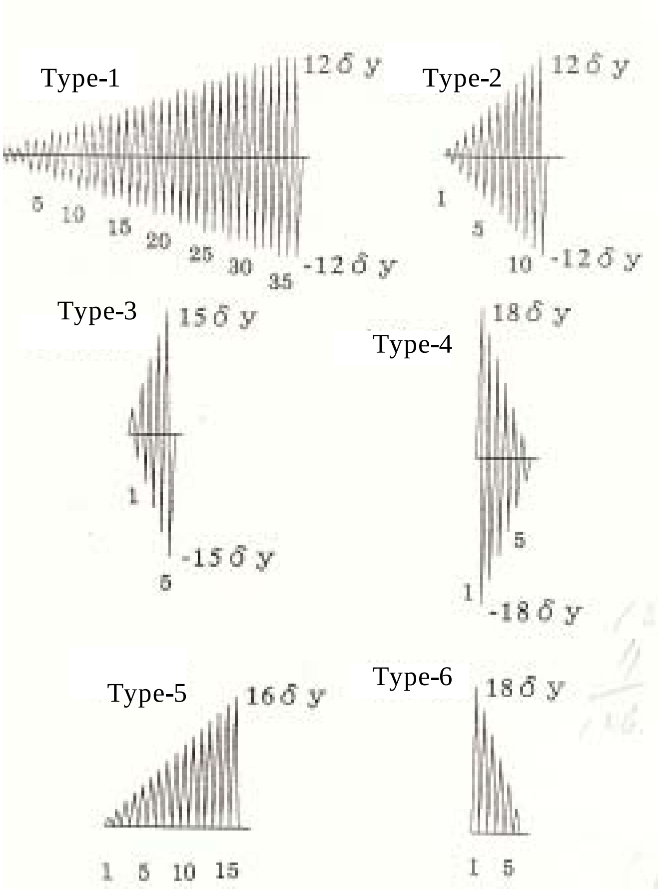

Fig.4.22 Loading Hystereses for Rectangular Columns

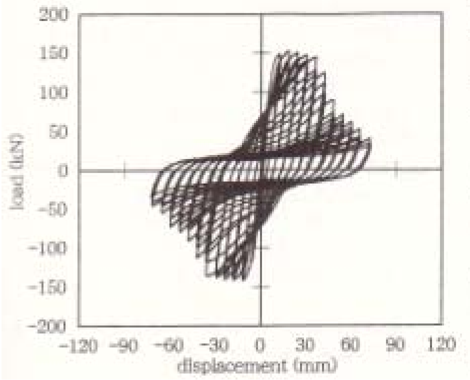

(a) Type 1 loading

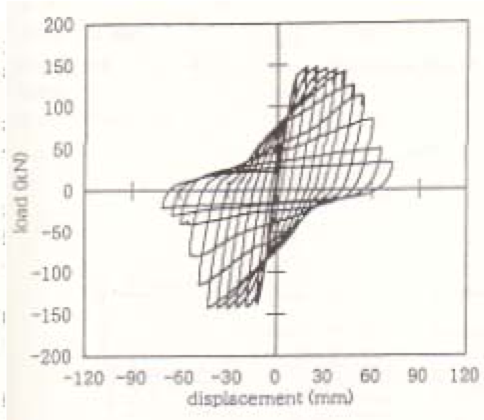

(b) Type 2 Loading

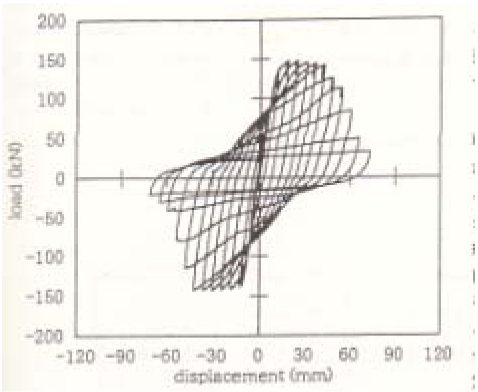

(c) Type 3 Loading

Fig.4.23 Effect of Number of Loading Cycles

0.98 MPa in the column. Based on calculation, the initial yield displacement u_{y0} is 6.0 mm which is nearly equal to 0.48 % drift.

Six loading hystereses as shown in Fig. 4.22 were used for test. Types 1, 2, and 3 are for studying the effect of number of load cycles. Type 4 represents a stepwise decrease loading. The displacement was reduced from 18 times yield displacement. Type 5 and Type 6 are for studying residual displacement in one direction.

Fig. 4.23 shows the effect of number of load cycles in the stepwise increasing loading. As the number of load step increases, the ultimate displacement decreases. Fig. 4.24 shows the lateral force vs. lateral displacement hysteresis for the stepwise decrease loading. Compared to Test 3, the restoring force on the first excursion toward $18u_{y0}$ is stable until $18u_{y0}$ (8.7 % drift) under the stepwise decrease loading, while the restoring force of the column under the stepwise increase starts to significantly deteriorate after $12u_{y0}$.

Fig. 4.25 shows hystereses of the lateral force vs. lateral displacement relation for the columns subjected to a loading only in one direction (Types 5 and 6). The difference of the stepwise decrease and increase loadings is also apparent in this comparison.

Since the lateral confinement of concrete is much less in the rectangular columns than the circular columns, the difference of loading scheme results in larger difference in the hysteretic behavior. This is important for deciding ultimate displacement of columns subjected to near-fields ground motions.

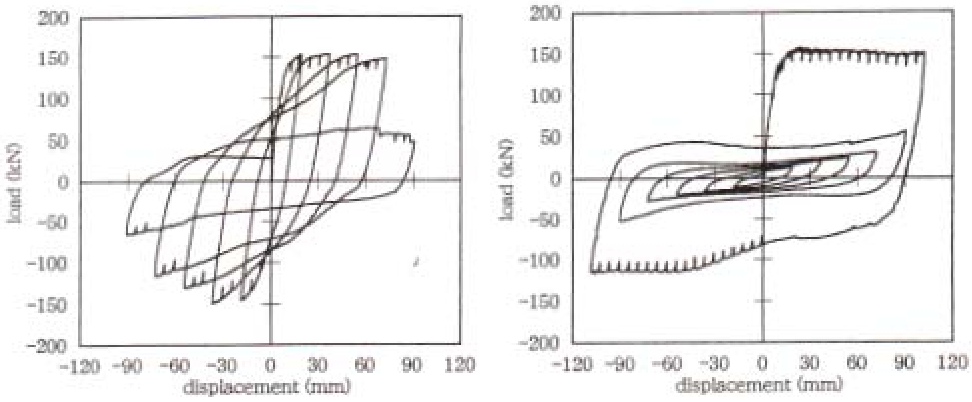

(a) Type 3 Loading (b) Type 4 Loading

Fig.4.24 Hystereses under Types 3 and 4 Loadings

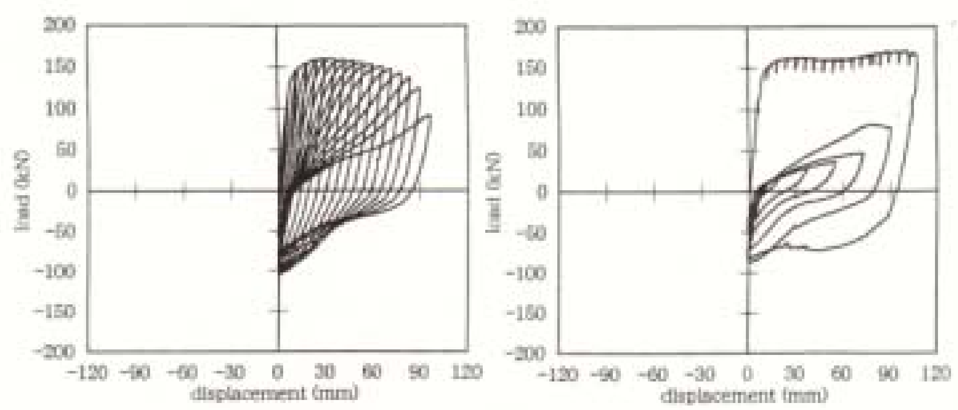

(a) Type 5 Loading (b) Type 6 Loading

Fig.4.25 Hystereses under Types 5 and 6 Loadings

2) Effect of Varying Axial Force

Reinforced concrete members are often subjected to lateral force under varying axial force. For example, a column in a pier consisting of several columns, a pile in a pile foundation consisting of group piles, and an arch rib of an arch bridge are subjected to bending under a varying axial force. Reinforce concrete columns subjected to varying axial force exhibit unique hysteretic behavior. An example of loading test for rectangular reinforced concrete columns (Sakai and Kawashima 2002) is described below.

The columns are 1.35 m tall (effective height) and have a section of 400 mm x 400 mm. Twenty D13 bars and D6 bars with an interval of 50 mm are provided for longitudinal and tie bars, respectively. The yield strength of D13 and D6 bars are 374 MPa and 363 MPa, respectively. The longitudinal reinforcement ratio and the volumetric tie reinforcement ratio are 1.58% and 0.79%, respectively. The concrete strength is between 22.9 and 23.0 MPa.

The columns were stepwise loaded in the lateral direction under four vertical loads; (1) constant compression axial load corresponding to 3 MPa, (2) constant tension axial load corresponding to 1 MPa, (3) varying axial load corresponding to 1 MPa (mean value) +/- 1

MPa, and (4) 1 MPa (mean value) +/- 2 MPa. They are called herein as CC, CT, V1, and V2 specimens. CT specimen was loaded under a constant tension axial force for clarifying the effect of axial load although it is unrealistic to design such a structural member in reality. The lateral displacement was stepwise increased such as 0.5% drift, 1% drift, 1.5% drift, …., until failure, and three load reversals were applied per step.

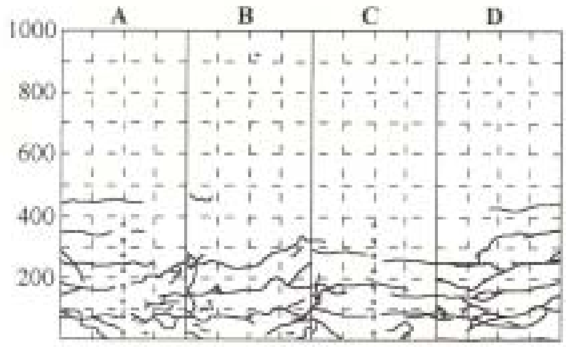

(a) CC Specimen after 3% Drift Loading

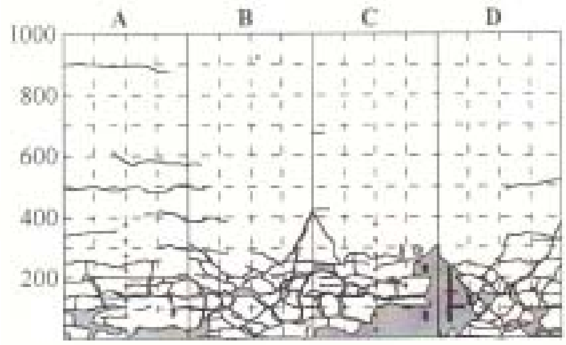

(b) CT Specimen after 4% Drift Loading

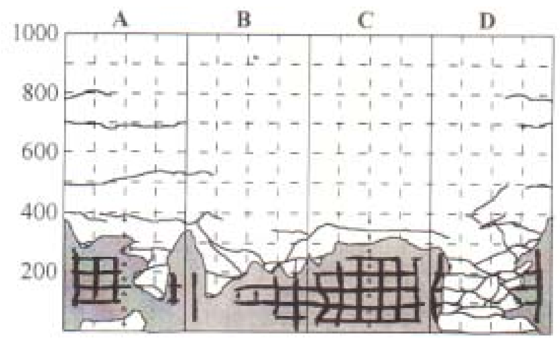

(c) V1 Specimen after 1st Cycle of 5% Drift Loading

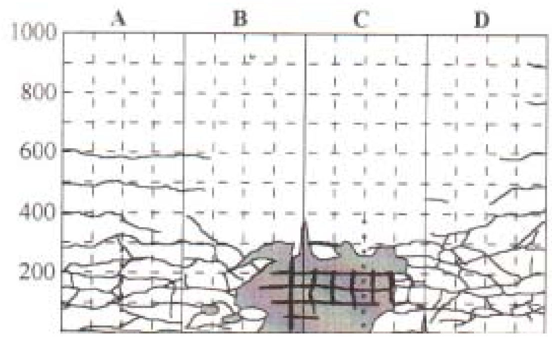

(d) V2 Specimen after 4% Drift Loading

Fig.4.26 Failure Mode at Typical Loading Steps

Fig. 4.26 shows failure modes at typical load steps. The columns were laterally loaded in A-C direction. It is noted that the axial load in compression increases when the column is laterally loaded toward C direction, and the axial load in compression decreases (The smallest axial stress of concrete is 0 in V1 and -1 MPa in V2) when the column is laterally loaded toward A direction. The failure of CC specimen progressed from spalling off of covering concrete, and outward buckling and rupture of longitudinal bars.

On the other hand, not only flexural cracks but also shear cracks occurred during 2.5% drift in the CT specimen. Fig. 4.27 shows this shear cracks at the plastic hinge. The shear cracks resulted in a as large as +/- 3 mm lateral shear movement of the upper column relative to the lower column block. The shear movement progressed to +/- 5 mm at 3% drift, +/- 9 mm at 3.5% drift, and +/- 12 mm at 4% drift. Extensive buckling of longitudinal bars start to occur at 5% drift. Being different from the simple outward buckling of longitudinal bars in the CC specimen, when the longitudinal bars are subjected to flexural tension, they are extended from buckled shapes due to not only flexural tension but also shear. As a consequence, the longitudinal bars yield complicated buckling modes.

In the V1 and V2 specimens, compression failure of concrete in the plastic hinge is always larger at C surface than A surface, since the flexural compression and the compression due to the vertical load are combined resulting in larger compression in the C surface than A surface.

Fig. 4.28 shows hysteresis loops of the lateral force vs. lateral displacement relations. Plus displacement represents the displacement toward C direction, where compression due to the vertical load increases in V1 and V2. In the CC specimen, the flexural strength is 174 kN and 161 kN in the positive and negative displacements, respectively. On the other hand, strength of CT specimen is only 97 kN and 92 kN in positive and negative displacements, respectively, which are nearly 55% on the flexural strength of CC specimen. As described above, the shear

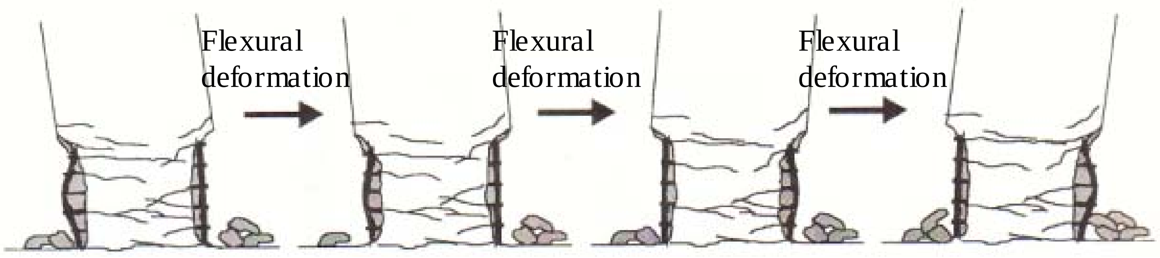

(a) Cyclic Loading under a Constant Compression (CC)

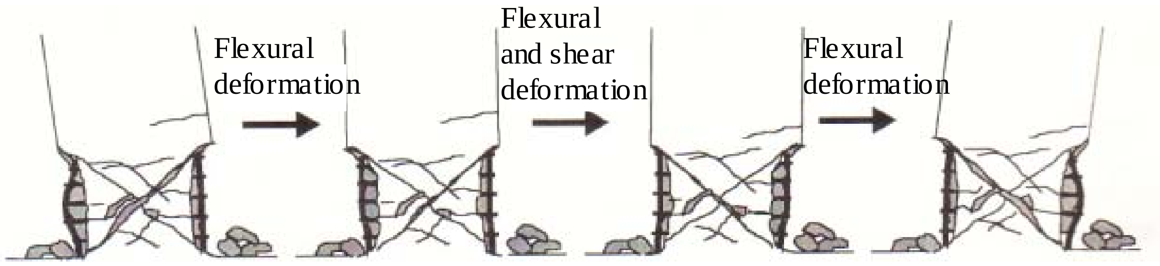

(b) Cyclic Loading under a Constant Tension (CT)

Fig.4.27 Failure mode at the Plastic Hinge Region

movement occurs along shear cracks, but this does not necessarily results in a significant deterioration of lateral restoring force. The lateral restoring force starts to deteriorate at 3.5-4% drift when covering concrete start to spall off. At 4.5% drift, the restoring force reduced to 50% of the maximum values, and the loading was terminated at 6 % drift since a longitudinal bar ruptured. At this stage, not only the covering concrete but also the core concrete suffered extensive failure at nearly 40% of its total sectional area. Among 20 longitudinal bars, one ruptured and 19 bars buckled in complicated modes. It is noted that a sudden deteriorate of lateral restoring force resulted from shear failure did not tale place until the end of the loading.

In the V1 and V2 specimens, restoring forces are always larger in positive lateral displacement (toward C surface) than negative lateral displacement (toward A surface). This is resulted by the increased compression due to the vertical load in the positive lateral displacement. It is noted however that deterioration of the restoring force is larger in the positive lateral displacement than the negative lateral displacement. The larger compression force at C surface in the positive lateral displacement results in earlier compression failure in this surface.

Fig. 4.29 compares a cycle of hysteresis loop of 4 specimens at loading displacements of 1.5%, 2.5% and 3.5%. The hystereses of the V1 and V2 specimens are close to the hysteresis of CC at the positive lateral displacement, while they are close to the hysteresis of CT in the negative lateral displacement. This can be explained by the combination of the flexural compression and the vertical load.

Fig. 4.30 shows the equivalent stiffness by Eq. (4.4) for the four specimens. Obviously the equivalent stiffness of CT specimens is significantly smaller than the equivalent stiffness of

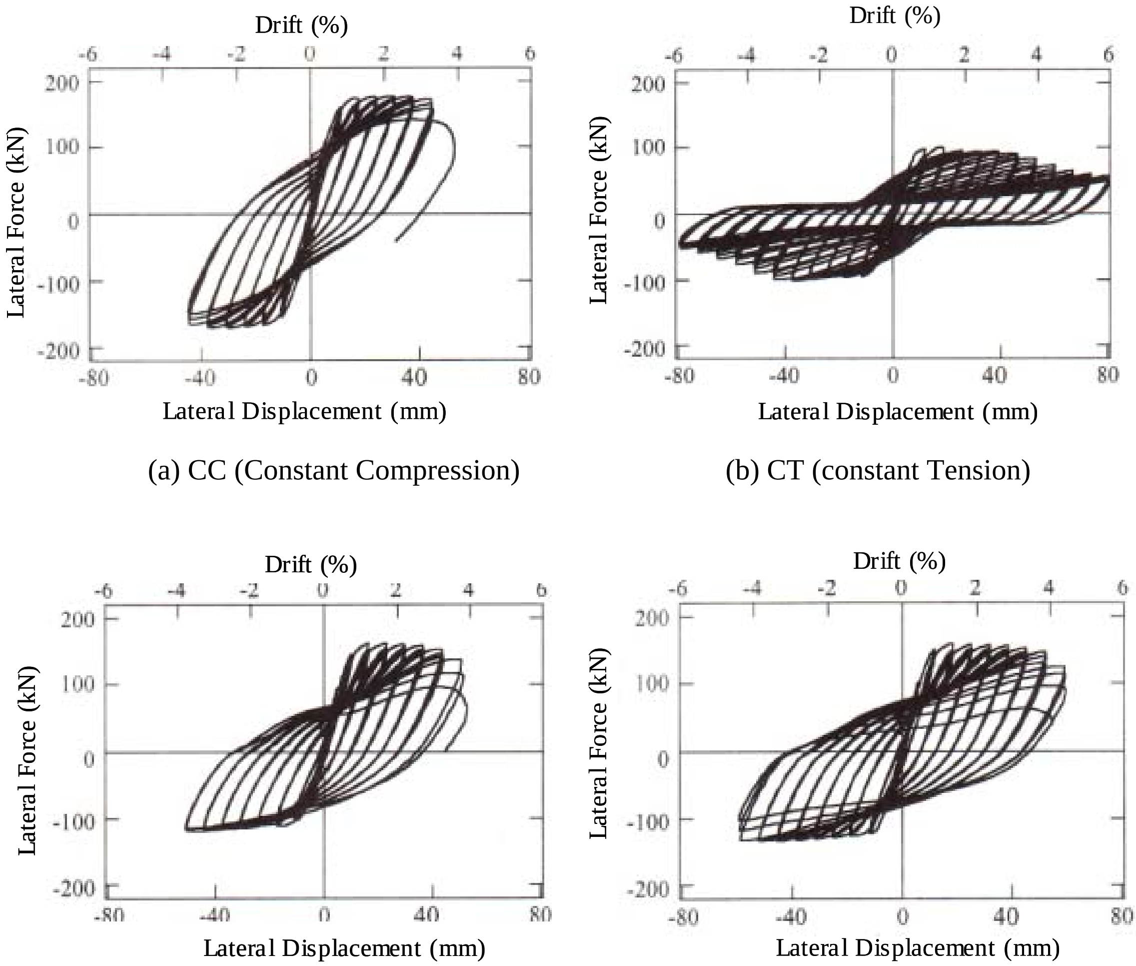

(a) CC (Constant Compression) (b) CT (constant Tension)

(c) V1 (Varying between 0 and 2 MPa) (d) V2 (Varying between -1 and 2.7 MPa)

Fig.4.28 Lateral Force vs. Lateral Displacement Hystereses under Various Vertical Loads

other specimens. Fig. 4.31 shows the energy dissipation at each loading step ΔW_i and the accumulated energy dissipation ΔW by Eqs. (4.6) and (4.7), respectively. Energy dissipation ΔW_i does not increase after 2% drift in the CT specimen, which results in significantly smaller accumulated energy dissipation ΔW in this specimen.

The lateral force vs. lateral displacement hystereses were analyzed using the fiber element analysis. The analytical model and the constitutive models for confined concrete and rebars presented in 4.2 were used here. To include the effect of strain hardening, the post yield stiffness of bars is assumed as 2% of the elastic stiffness.

Fig. 4.32 shows the computed and experimental hystereses for the four specimens. The flexural strength as well as unloading and reloading paths are well predicted by the analysis for CC, V1 and V2 specimens. Since shear deformation and the early deterioration of core concrete and bars cannot be accounted for in the analysis for the CT specimen, the accuracy is for in this case.

3) Effect of Bilateral Loading

Although it is common to consider the lateral loading only in one direction in seismic design of bridges, bridges are subjected to two lateral loadings in reality. The effect of bidirectional loading is especially important in skewed and curbed bridges. Reinforced concrete columns

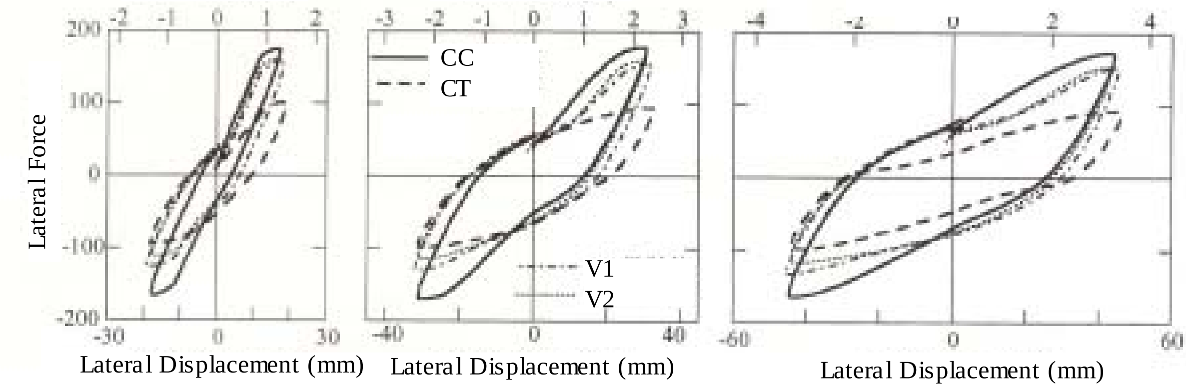

(a) 1.5% Drift (b) 2.5% Drift (c) 3.5% Drift

Fig. 4.29 Comparison of Hysteresis loops

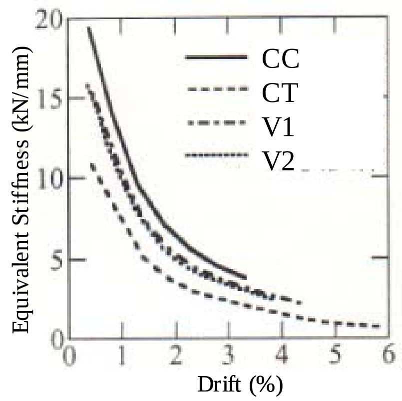

Fig. 4.30 Equivalent Stiffness

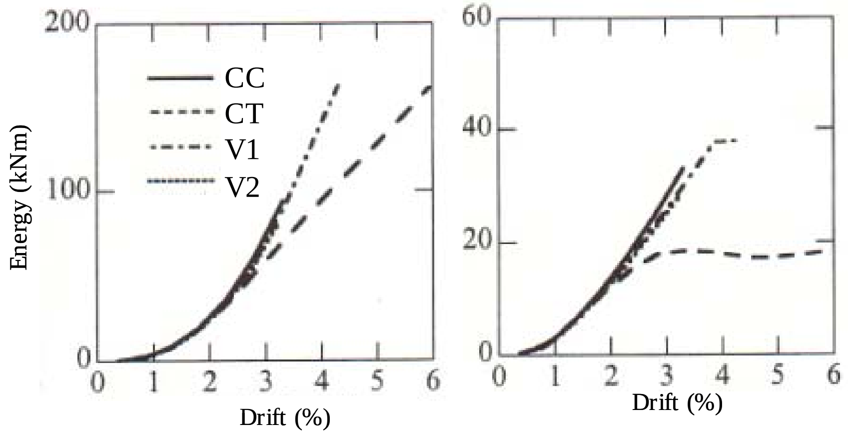

(a) Energy Dissipation per Cycle (b) Accumulated Energy Dissipation

Fig. 4.31 Energy Dissipation

subjected to bilateral loading exhibits interesting hysteretic behavior. A cyclic loading test for this effect is described below. Five 1.35 m tall (effective height) square reinforced concrete columns with a section of 400 mm x 400 mm were used for test. Sixteen D13 (SD295A) longitudinal bars and D6 (SD295A) tie bars at 50 mm interval were provided. The longitudinal ratio and the volumetric tie reinforcement ratio are 1.27% and 0.79%,

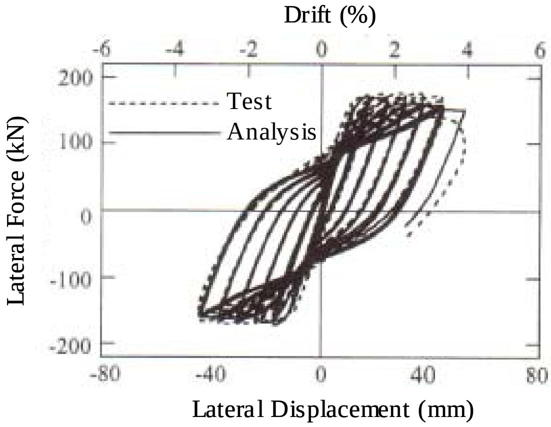

(a) CC (Constant Compression)

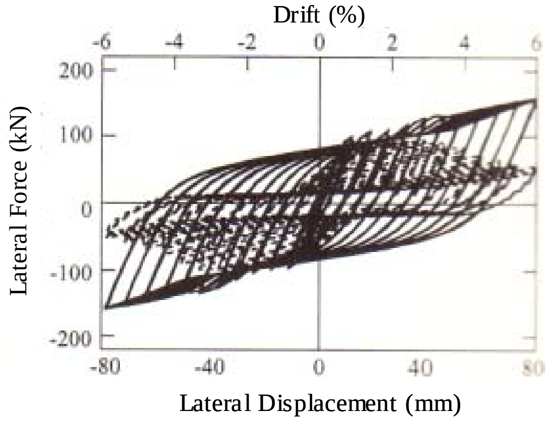

(b) CT (constant Tension)

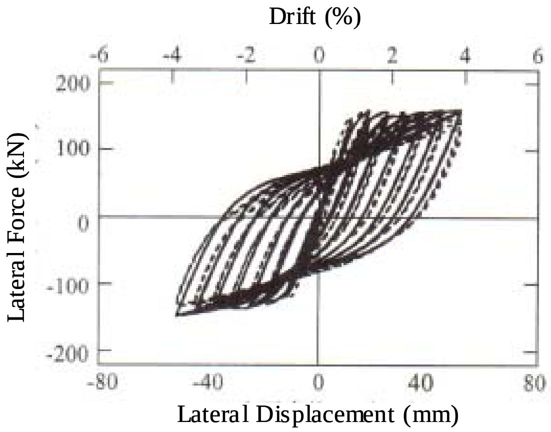

(c) V1 (Varying between 0 and 2 MPa)

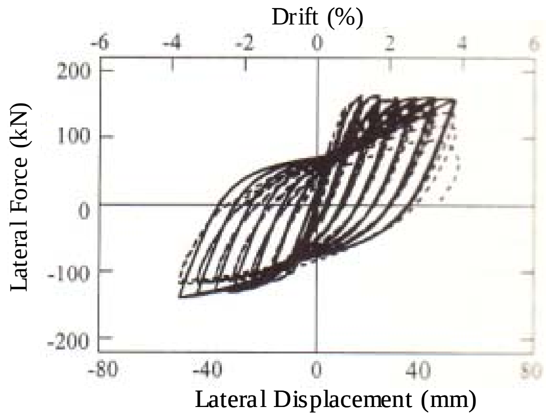

(d) V2 (Varying between -1 and 2.7 MPa)

Fig.4.32 Lateral Force vs. Lateral Displacement Hystereses using Fiber Element Analysis

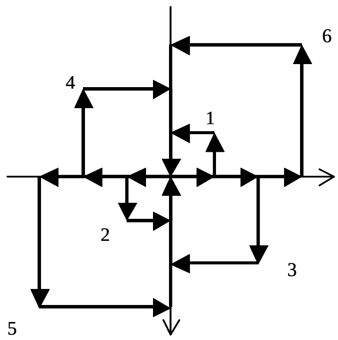

Fig. 4.33 Rectangular Loading Hysteresis

respectively. The concrete strength was between 26.2 and 31.3 MPa. The columns were loaded under a constant vertical load of 160 kN, which corresponded to a stress of 1MPa, using five lateral loading modes; (1) unilateral, (2) 45 degree oblique to column axis, (3) rectangular orbit as shown in Fig. 4.33, (4) circular orbit, and (5) ellipsis orbit. In the rectangular orbit, the column was loaded in one direction, and then keeping the displacement

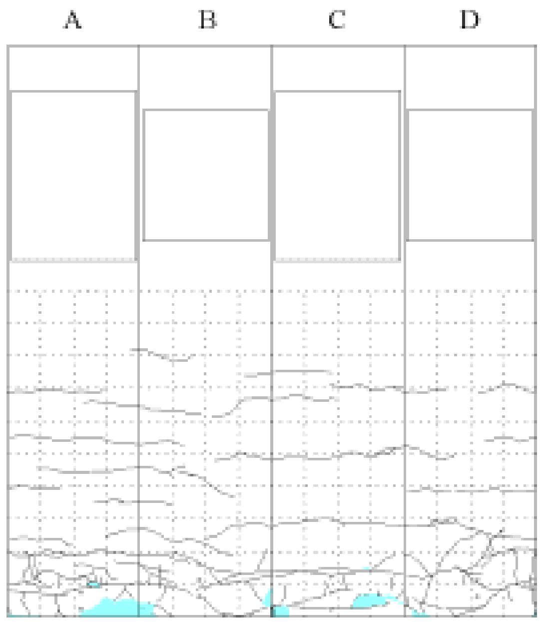

(a) Unilateral Loading

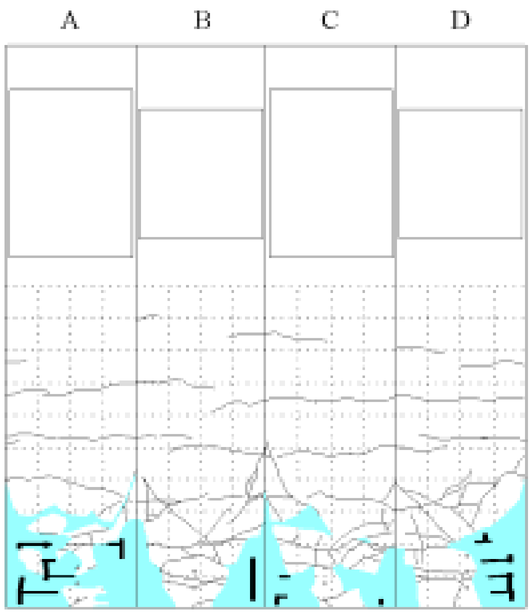

(b) Rectangular Orbit

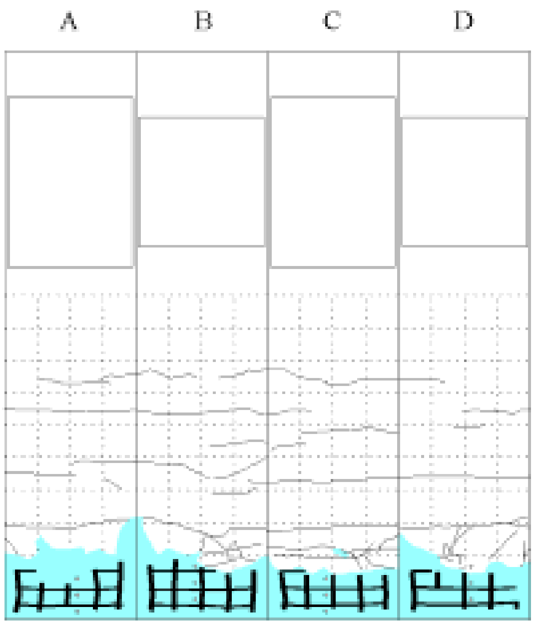

(c) Circular Orbit

Fig. 4.34 Failure Modes of Columns Subjected to Unilateral and Bilateral Loadings after 3.5% Drift Loading was completed

in this direction, the column was loaded in the other direction. After unloading from a peak displacement in both directions, the column was loaded in the opposite directions. The lateral loading displacement was stepwise increased from 0.5% drift with an increment of 0.5% drift until failure. Test results are presented below only for the unilateral loading and bilateral loading with the rectangular and circular orbits.

Fig. 4.34 shows failure modes of columns subjected to the unilateral and bilateral

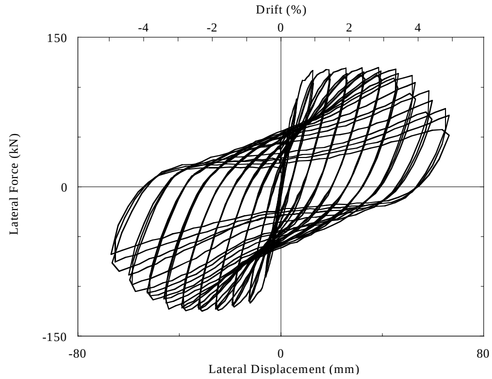

(1) Unilateral Loading

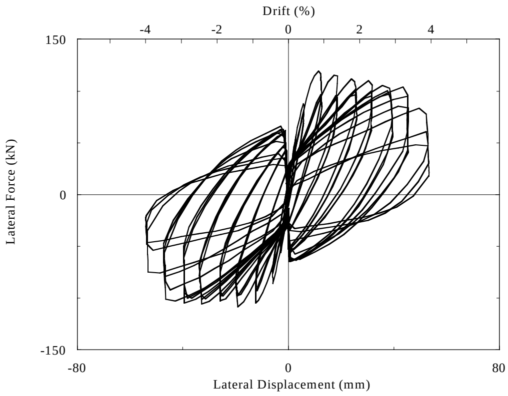

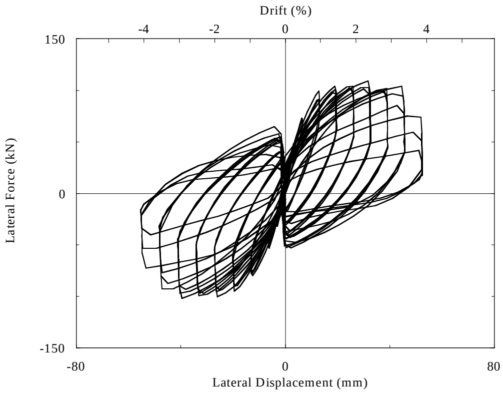

(a) A-C Direction (b) B-D Direction

(2) Rectangular Orbit

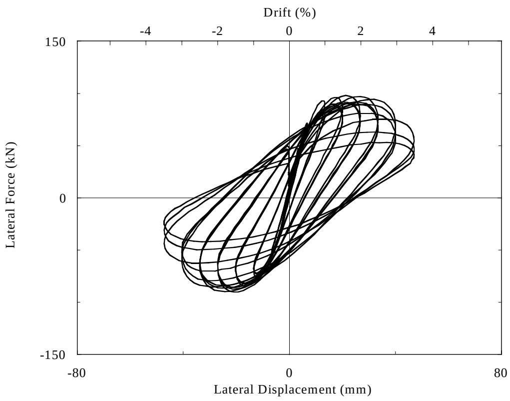

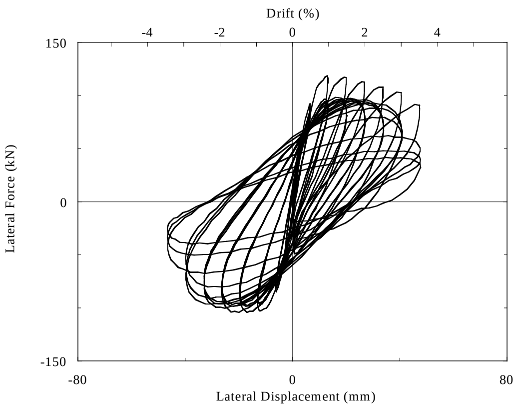

(a) A-C Direction (b) B-D Direction

(3) Circular Orbit

Fig. 4.35 Lateral Force vs. Lateral Displacement Hystereses of Columns Subjected to Unilateral and Bilateral Loadings

loadings with the rectangular and the circular orbits after 3.5% drift loading was completed. Failure of the column subjected to the unilateral loading (A-C direction) progressed as shown in Fig. 4.14. The compression failure of concrete is concentrated at A and C surfaces. On the other hand, the failure of column under the rectangular orbit starts to take place at the corners.

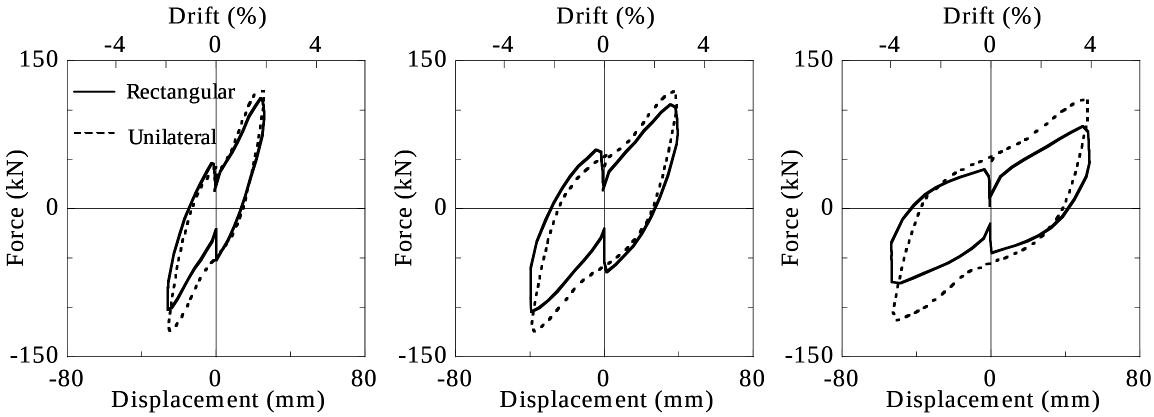

(1) Rectangular Orbit (A-C Direction)

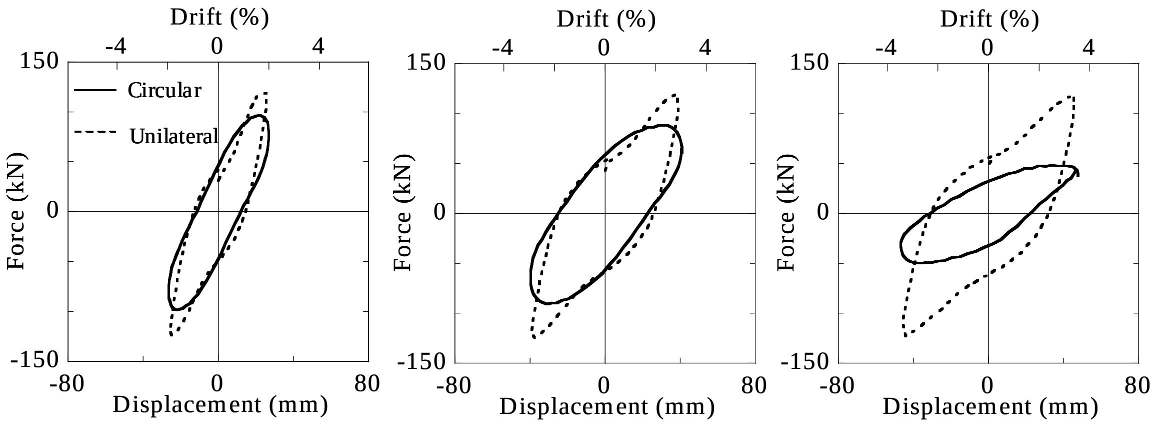

(a) A-C Direction (b) B-D Direction

(2) Circular Orbit (A-C Direction)

Fig. 4.36 Comparison of Hysteresis Loops between Unilateral and Bilateral Loadings

Combination of compression forces due to the bilateral loading results in larger compression force to take place at the corners. The compression failure propagates from the corners to the four surfaces as the loading displacement increases. This has occurred by 3.5% drift in the column subjected to the circular orbit. Extensive compression failure as well as complex local buckling of longitudinal bars has occurred until 3.5% drift in this column.

Fig. 4.35 shows the lateral force vs. lateral displacement hystereses for three columns. The hystereses are presented for two directions in the columns subjected to the bilateral loading. Pinching is observed at small displacement under the rectangular loading, because the restoring force in one direction deteriorates while the column is loaded in the other direction. On the other hand, the hysteresis under the circular orbit is round around peak displacements. Fig. 4.36 compares the hysteresis loops for a single load excursion. Restoring forces as well as unloading and reloading stiffness deteriorate earlier under the bilateral loading than the unilateral loading. Fig. 4.37 compares envelops of the lateral force vs. lateral displacement hystereses. Extensive deterioration of the restoring forces occurs when the columns are subjected to the bilateral loading. Significant deterioration of the column tends to results in a larger deck displacement. It is important to note that ignoring the bilateral loading underestimates the bridge response.

Hysteretic behavior of the columns under the bilateral loading was analyzed using the

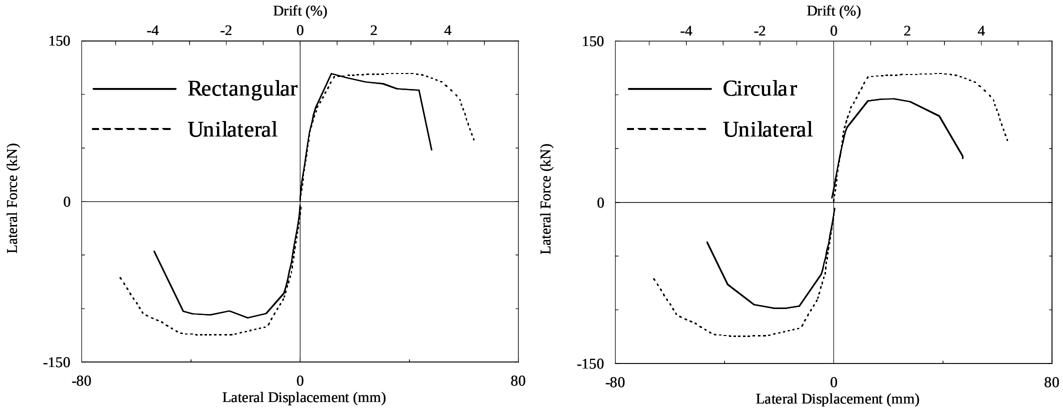

(a) Rectangular Orbit (A-C Direction) (b) Circular Orbit (A-C Direction)

Fig. 4.37 Comparison of Envelopes between Unilateral and Bilateral Loadings

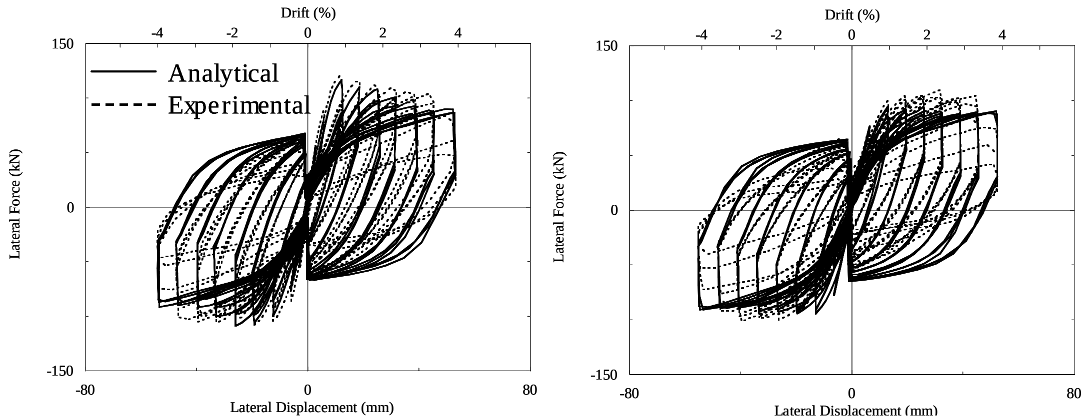

(a) A-C Direction (b) B-D Direction

Fig. 4.38 Comparison of Computed and Experimental Hysteresis (Rectangular Orbit)

fiber element analysis. The constitutive models for confined concrete by Hoshikuma, Kawashima, Nagaya and Taylor (1997) and Sakai and Kawashima (2000), and the constitutive model of bars by Meneggoto and Pinto (1973) were used here. Fig. 4.38 shows a correlation of the lateral force vs. lateral displacement hystereses under the rectangular orbit. Fig. 4.39 shows a detailed comparison of the hystereses between the experiment and analysis for specific loading displacements. Accuracy of the analysis is acceptable until 3.5% drift. Since the effect of buckling of bars and the extensive failure of concrete is not accounted for in analysis, the accuracy decreases over 3.5% drift. In a similar way, Figs. 4.40 and 4.41 shows a correlation of the hysteresis under the circular orbit. Accuracy is acceptable until 3% drift loading.

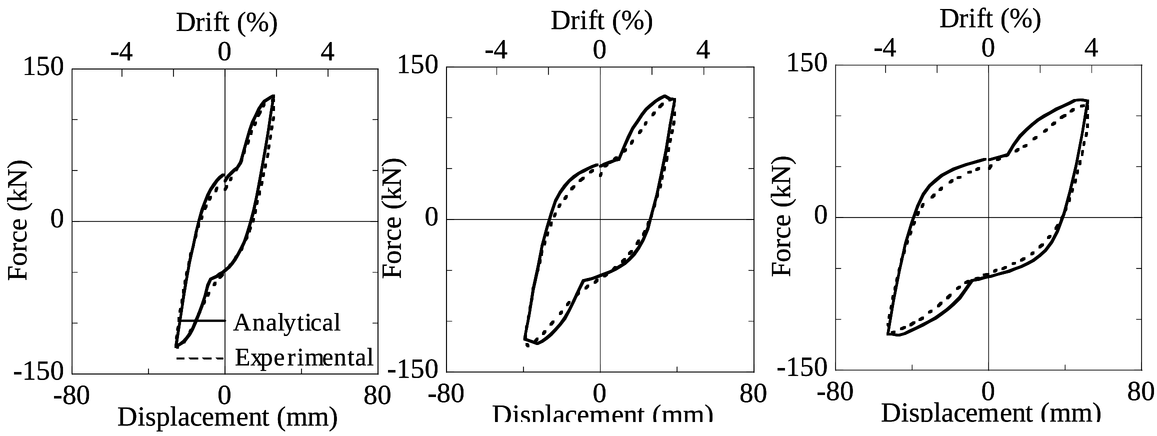

(a) 2% Drift (b) 3% Drift (c) 4% Drift

Fig.4.39 Comparison of Computed and Experimental Hysteresis (Rectangular Orbit)

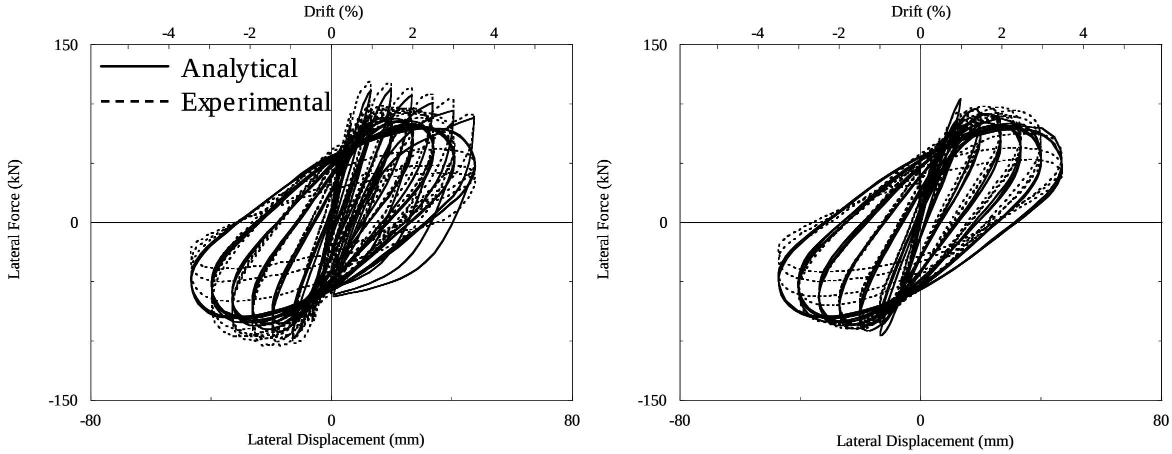

(a) A-C Direction (b) B-D Direction

Fig. 4.40 Comparison of Computed and Experimental Hysteresis (Circular Orbit)

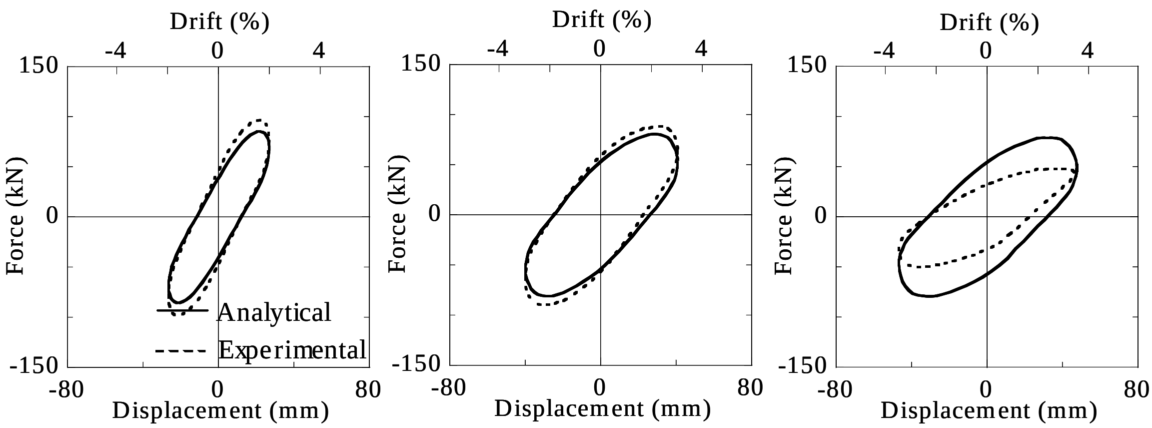

(a) 2% Drift (b) 3% Drift (c) 3.5% Drift

Fig.4.41 Comparison of Computed and Experimental Hysteresis (Circular Orbit)